On forced coastal trapped waves at low latitudes in a stratified ocean

by R. D. Romea[1] and J. S. Allen[1]

ABSTRACT

The response on the continental shelf and slope of a baroclinic ocean to driving by an alongshore wind stress at the coast ($\tau^{y}_{(0)}$) and by barotropic and baroclinic wind forced interior motions is studied as a function of latitude. A two layer linear model is utilized. Solutions are obtained in two ways: (1) the cross-shelf eigenfunctions of the unforced problem are used to derive a forced first order wave equation for the alongshore and time dependent behavior of each eigenfunction in an f-plane model; (2) the shelf response is obtained directly using an idealized wind stress forcing with sinusoidal dependence on time and on the horizontal spatial coordinates in a β-plane model. The cross-shelf eigenfunctions consist of an internal Kelvin wave (IKW) and a series of shelf waves (SW) whose vertical structure depends on latitude. For mid-latitudes the SW modes are barotropic while for low latitudes they are bottom trapped. For forcing at low latitudes, the IKW mode is efficiently excited by $\tau^{y}_{(0)}$, while the SW modes are not efficiently excited. The relative excitation of the SW modes with respect to the IKW mode is greater away from lower latitudes. For mid-latitudes, the forced SW mode energy is comparable or greater than the forced IKW mode energy, and barotropic interior motions force energetic SW modes. Using method (2), the relative effects of interior barotropic motions and of $\tau^{y}_{(0)}$ are compared. For forcing by a sinusoidal traveling wave at mid-latitudes, the shelf circulation is predominantly due to the local alongshore wind stress. Near the shelf break, however, the effects of motions in the interior may be felt, and phase differences between the response forced by $\tau^{y}_{(0)}$ and by interior barotropic motion may lead to cross-shelf phase lags. For lower latitudes, interior effects are larger relative to direct wind stress as a driving mechanism for motion in the lower layer. For latitudes $<10°$, the forced response in the lower layer due to interior motions may be comparable to or greater than the local wind forced response. For decreasing frequency, the interior motion penetrates less effectively onto the shelf-slope region, and the coastal wind forced response is confined more closely to the coast. For these cases, motion near the slope-interior junction will be driven predominantly by offshore circulations.

1. Introduction

The response on a continental shelf and slope to forcing by wind stress and by interior oceanic motion will vary with latitude. This response will also depend on the stratification, the shelf-slope topography, and the nature of the motion in the interior ocean.

1. School of Oceanography, Oregon State University, Corvallis, Oregon 97331, U.S.A.

Recent observations from the Coastal Upwelling Ecosystems Analysis (CUEA) experiment on the continental shelf and slope off the coast of Peru (Brink *et al.*, 1978; Smith, 1978) at 10-15S indicate strong poleward propagating wavelike motions in the alongshore component of the currents which are typically not well correlated with the local alongshore component of the wind stress. Motivated by these observations, we study the characteristics of forced long waves trapped over a continental shelf and slope as a function of latitude and we investigate the interior oceanic motion as a possible source for the observed propagating energy. We consider a linear inviscid two layer ocean with a continental shelf and slope along the eastern boundary. A response may be forced on the shelf by the wind directly through the alongshore component of the wind stress at the coast and indirectly through the interaction with the shelf of motions forced in the interior ocean by the wind stress curl.

We first solve the forced problem in terms of cross-shelf eigenfunctions of the unforced problem, using an f-plane. With this approach, a first order wave equation may be obtained for the alongshore and time-dependent behavior of each wave mode. This method is particularly well suited for initial-value problems where it shows how the forced flow on the shelf develops as each wave mode responds to the forcing. Since the phase velocities vary and the eigenfunctions change structure as a function of latitude, the mid-latitude forced response, aspects of which have been discussed by Gill and Schumann (1974) and Allen (1976a), will differ from the low latitude forced response.

The problem is also approached in another way. For an idealized wind stress forcing, with sinusoidal dependence on time and on the horizontal spatial coordinates (e.g., a traveling wave), the onshore-offshore structure of the solutions on the shelf may be obtained directly. These solutions are particularly well suited for determining the relative importance of the various mechanisms for forcing shelf circulations. For example, the offshore dependence of the solutions forced by the alongshore component of the wind stress at the coast and by the interior wind forced batrotropic and baroclinic motions may be compared as a function of latitude, forcing frequency and wavenumber. Since the solutions change character for forcing at very low frequency (Section 5b), the β-effect is included in the analysis to establish the validity of the f-plane solutions presented in Sections 3-5.

2. Formulation

We consider a north-south oriented boundary on the eastern side of a two layer β-plane ocean, where Cartesian coordinates (x', y', z'), are utilized,[2] with x' positive in the offshore direction (the coastline is at $x' = 0$), y' positive *southward*, and z'

2. In this and the following sections, dimensional variables for which a nondimensional counterpart will be defined are denoted with primes.

positive vertically upward. Stratification is modelled by two layers of homogeneous fluid of different density, with the heavier fluid on the bottom. The top surface is bounded by a rigid lid. The upper layer fluid has density ρ_1, and a constant undisturbed depth H'_1. The lower layer fluid has density ρ_2 and a variable undisturbed depth $H'_2 = H'_2(x', y')$. The total depth is $H' = H'_1 + H'_2$. The difference in density $\Delta\rho = \rho_2 - \rho_1$ is assumed to be small, $\Delta\rho/\rho_2 << 1$. Along the boundary there is a continental shelf and slope topography which is confined to the region $0 \leqslant x' \leqslant L_S$. In the interior ($x' \geqslant L_S$), the depth is constant, $H' = H'_0 = H'_1 + H'_{20}$.

Dimensionless variables are formed in the following manner:

$$
\begin{aligned}
&(x, y) = (x', y')/L,\ z = z'/H'_0,\ \tilde{t} = \tilde{t}' f_0,\\
&(u_i, v_i) = (u'_i, v'_i)/U,\ w_i = w'_i L/(H'_0 U),\\
&p_1 = [p'_1 + \rho_1 g(z' - H'_0)]/(\rho_1 U f_0 L),\\
&p_2 = [p'_2 + \rho_2 g(z' - H'_{20}) - \rho_1 g H'_1]/(\rho_2 U f_0 L),\\
&h = h'\, g\Delta\rho/(\rho_2 U f_0 L),\\
&(H_1, H_2, H) = (H'_1, H'_2, H')/H'_0,\\
&\boldsymbol{\tau} = \boldsymbol{\tau}'/(U\rho_2 f_0 H_1),\\
&f = (f_0 - \beta' y')/f_0 = 1 - \beta y,
\end{aligned}
\tag{2.1}
$$

where $i = 1, 2$ refers to the upper and lower layer, respectively. The variables (u', v', w') are the velocity components in the (x', y', z') directions, p' is the pressure, $\tilde{t}'$ is time, L is a characteristic horizontal alongshore scale (the dimensional alongshore wavelength $\lambda' = 2\pi L$), U is a characteristic horizontal velocity [$U = \tau'_0/(\rho_2 f_0 H_1)$, where τ'_0 is a characteristic wind stress], g is the acceleration of gravity, $\boldsymbol{\tau}'$ is the surface wind stress vector with (x', y') components ($\tau^{x'}$, $\tau^{y'}$), f_0 is the value of the Coriolis parameter at a reference latitude and $\beta = \beta' L/f_0$. $h = p_2 - p_1$ is the dimensionless perturbation interface height.

The resulting linear, depth integrated continuity and momentum equations for each layer are (subscripts x, y, $\tilde{t}$ denote partial differentiation)

$$(H_1 u_1)_x + (H_1 v_1)_y = S^{-1} h_{\tilde{t}}, \tag{2.2a}$$

$$u_{1\tilde{t}} - f v_1 = -p_{1x} + \tau^x, \tag{2.2b}$$

$$v_{1\tilde{t}} + f u_1 = -p_{1y} + \tau^y, \tag{2.2c}$$

$$(H_2 u_2)_x + (H_2 v_2)_y = -S^{-1} h_{\tilde{t}}, \tag{2.2d}$$

$$u_{2\tilde{t}} - f v_2 = -p_{2x}, \tag{2.2e}$$

$$v_{2\tilde{t}} + f u_2 = -p_{2y}, \tag{2.2f}$$

where $S = (NH'_0/f_0 L)^2$ is the stratification parameter and $N^2 = g\Delta\rho/(\rho_2 H'_0)$ is the square of the Brunt-Väisälä frequency.

If (2.2a) and (2.2d) are combined, a streamfunction may be defined, such that

$$\psi_y = u_1 + (H_2/H_1)\, u_2, \tag{2.3a}$$

$$-\psi_x = v_1 + (H_2/H_1)\, v_2. \tag{2.3b}$$

The general governing equations for the perturbation interface height h and the streamfunction ψ may be obtained from (2.2) (Allen, 1975) and are:

$$\begin{aligned}[\psi_{xx} + \psi_{yy} - (H_x/H)\psi_x - (H_y/H)\psi_y]_t - \beta\psi_x \\ = (H_x/H)\,(h_y - f\psi_y + \tau^y) - (H_y/H)\,(h_x - f\psi_x + \tau^x) \\ - (\tau_x{}^y - \tau_y{}^x),\end{aligned} \tag{2.4a}$$

$$\begin{aligned}[h_{xx} + h_{yy} + a(H_x/H)h_x + a(H_y/H)h_y - (SH)^{-1}\, Dh \\ - (\beta/f)\,(h_x - h_y)]_t - \beta h_x \\ = -a(H_x/H)\,[fh_y - D\psi_y + f\tau^y + \tau_t{}^x] \\ - a(H_y/H)\,[fh_x - D\psi_x + f\tau^x - \tau_t{}^y] \\ + \beta\tau^x - f(\tau_x{}^y - \tau_y{}^x) - \\ (\tau_x{}^x + \tau_y{}^y)_t,\end{aligned} \tag{2.4b}$$

where $D = f^2 + (\partial^2/\partial t^2)$, $a = H_1/H_2$.

The following assumptions are utilized:

1) restrict the topography to have no alongshore variations, so that $H = H(x)$ only;

2) assume $\beta << 1$;

3) restrict attention to motions on a time scale δ_t large compared with an inertial period, i.e., $\delta_t >> f^{-1}$;

4) assume the scale of the wind stress and therefore the scale of the interior motion and the alongshore scale of the motion on the shelf is 0(1);

5) assume the interior Rossby radius of deformation [defined in (2.8)] is much smaller than the 0(1) alongshore scale,

$$\bar{\delta}_{RI} << 1; \tag{2.5a}$$

6) assume the dimensionless width of the shelf-slope region δ is also much smaller than the 0(1) alongshore scale,

$$\delta << 1; \tag{2.5b}$$

7) assume that the small parameters δ, $\bar{\delta}_{RI}$, and β are, in general, of the same order-of-magnitude, i.e.,

$$0(\delta) = 0(\bar{\delta}_R) = 0(\beta). \tag{2.5c}$$

It is convenient to define a new cross-shelf variable and Rossby radius

$$\xi = x/\delta,\ \delta_R = \tilde{\delta}_R/\delta, \tag{2.6a}$$

and an associated time scale

$$t = \tilde{t}\delta. \tag{2.6b}$$

With the above assumptions the equations for the interior, where $H_x = 0$, are

$$\delta(\tilde{\psi}_{xx} + \tilde{\psi}_{yy})_t - \beta\tilde{\psi}_x = -(\tau_x{}^y - \tau_y{}^x), \tag{2.7a}$$

$$\delta(\tilde{h}_{xx} + \tilde{h}_{yy} - \tilde{\delta}_{RI}{}^{-2}\,\tilde{h})_t - \beta\tilde{h}_x = -f(\tau_x{}^y - \tau_y{}^x), \tag{2.7b}$$

where a tilda superscript denotes an interior variable. The interior Rossby radius, which is the natural offshore decay scale for baroclinic disturbances, is given by

$$\tilde{\delta}_R{}^2(\xi = 1) = \tilde{\delta}_{RI}{}^2 = f^{-2}S\tilde{H}_I\,, \tag{2.8a}$$

where

$$\tilde{H}(\xi) = H_1H_2/H \text{ and } \tilde{H}_I = \tilde{H}(\xi = 1). \tag{2.8b,c}$$

Equations (2.7a) for the barotropic interior motion and (2.7b) for the baroclinic interior motion are uncoupled and may be solved separately, subject to the proper boundary conditions.

At $x = \delta$, the junction of the interior and the shelf-slope region, the matching conditions, which follow from the continuity of mass flux and pressure, are

$$\tilde{h}(x = \delta) = h(\xi = 1), \tag{2.9a}$$

$$\tilde{h}_{xt}(x = \delta) = \delta^{-1}h_{\xi t}(\xi = 1), \tag{2.9b}$$

$$\tilde{\psi}_y(x = \delta) = \psi_y(\xi = 1), \tag{2.9c}$$

$$\tilde{\psi}_{xt}(x = \delta) = \delta^{-1}\psi_{\xi t}(\xi = 1). \tag{2.9d}$$

We expand $\tilde{\psi}$ in an asymptotic series, i.e.,

$$\tilde{\psi} = \delta^{-1}(\tilde{\psi}_0 + \delta\tilde{\psi}_1 + \ldots), \tag{2.10}$$

where the leading order is suggested by (2.7a). With this representation, (2.7a) is

$$(\tilde{\psi}_{0xx} + \tilde{\psi}_{0yy})_t - \beta\delta^{-1}\,\tilde{\psi}_{0x} = -(\tau_x{}^y - \tau_y{}^x). \tag{2.11}$$

The interior variable $\tilde{h}$ is conveniently written as two terms,

$$\tilde{h} = \tilde{h}_P + \tilde{h}_B, \tag{2.12}$$

where, from (2.7b) and with assumption (2.5a),

$$\delta\tilde{\delta}_{RI}{}^{-2}\,\tilde{h}_{Pt} + \beta\tilde{h}_{Px} = f(\tau_x{}^y - \tau_y{}^x), \tag{2.13}$$

and

$$(\tilde{h}_{Bxx} - \tilde{\delta}_{RI}{}^{-2}\,\tilde{h}_B)_t - \delta^{-1}\,\beta\tilde{h}_{Bx} = 0. \tag{2.14}$$

The variable $\tilde{h}_P$ is an approximate particular solution for the interior baroclinic

field forced by a wind stress curl with $\bar{\delta}_{RI} << 1$, whereas $\bar{h}_B$ is an approximate homogeneous solution which is added to $\bar{h}_P$ so that $\bar{h}$ satisfies the boundary conditions. Except for very low frequency motion, $\omega << \frac{1}{2}\ \beta\delta_{RI}$, the second term in (2.13) and the last term in (2.14) are small with respect to the other terms, and $\bar{h}_B$ in (2.14) represents the interior extension of a coastally trapped internal Kelvin wave. For very low frequency forcing, the third term in (2.11) and the second term in (2.13) balance the wind stress curl, resulting in an interior Sverdrup balance.

Expansions of the form

$$\psi = \psi_0 + \delta\psi_1 + \ldots, \tag{2.15a}$$

$$h = h_0 + \delta h_1 + \ldots, \tag{2.15b}$$

are assumed for the shelf. Since the interface perturbation h over the shelf due to the interior solution will consist of the interior interface deformation $\bar{h}_P$ $(x = 0)$, with a boundary layer correction to satisfy the boundary condition at $\xi = 0$, it is convenient to define a new shelf variable $\hat{h}$, where

$$h = \bar{h}_{P(0)} + \hat{h}, \tag{2.16}$$

(where the subscript (0) denotes evaluation at $x = 0$).
Using (2.5a,b), (2.6a,b), and (2.16), the lowest order equations for the shelf variables become

$$\begin{aligned}(\psi_{0\xi\xi} - \delta_B{}^{-1}\psi_{0\xi})_t - \delta_B{}^{-1}(\hat{h}_y - f\psi_{0y}) &= \delta_B{}^{-1}(\tau_{(0)}{}^y + \bar{h}_{Py(0)}) \\ &\quad -\delta(\tau_{x(0)}{}^y - \tau_{y(0)}{}^x) + \beta\psi_{0\xi},\end{aligned} \tag{2.17a}$$

$$\begin{aligned}&(\hat{h}_{\xi\xi} + a\delta_B{}^{-1}\hat{h}_\xi - \delta_R{}^{-2}\hat{h})_t + a\delta_B{}^{-1}f(\hat{h}_y - f\psi_{0y}) \\ &= -a\delta_B{}^{-1}f(\tau_{(0)}{}^y + \bar{h}_{Py(0)}) - f\delta(\tau_{x(0)}{}^y - \tau_{y(0)}{}^x) + \beta\hat{h}_\xi,\end{aligned} \tag{2.17b}$$

where $\delta_B{}^{-1}(\xi) = H_\xi/H$ and where $\delta_R{}^2(\xi) = f^{-2}\, S\bar{H}(\xi)\ \delta^{-2}$. The last two terms in (2.17a,b) are $0(\delta/\omega)$ and $0(\beta/\omega)$ with respect to terms on the left hand sides and are neglected in general, except in the limit $\omega \to 0$.

The velocities on the shelf may be obtained for each layer from ψ_0 and $\hat{h}$. They are

$$u_1 = H^{-1}H_1[\psi_{0y} + f^{-2}a^{-1}(f\hat{h}_y + \hat{h}_{\xi t}) + (af)^{-1}(\tau_{(0)}{}^y + \bar{h}_{P(0)y})], \tag{2.18a}$$

$$u_2 = H^{-1}H_1[\psi_{0y} - f^{-2}(f\hat{h}_y + \hat{h}_{\xi t}) - f^{-1}(\tau_{(0)}{}^y + \bar{h}_{P(0)y})], \tag{2.18b}$$

$$v_1 = (\delta H)^{-1}H_1[-\psi_{0\xi} - (af)^{-1}\hat{h}_\xi], \tag{2.18c}$$

$$v_2 = (\delta H)^{-1}H_1[-\psi_{0\xi} + f^{-1}\hat{h}_\xi], \tag{2.18d}$$

where (2.5b) has been used in the derivation of (2.18c,d). Eqs. (2.18c,d) imply that the alongshore component of the velocity is in geostrophic balance.

The boundary conditions at the coast, which follow from the requirement that $u_1 = u_2 = 0$ and (2.18) are

$$\psi_{0y} = 0 \text{ at } \xi = 0, \tag{2.19a}$$

$$f\hat{h}_y + \hat{h}_{\xi t} = -f(\tau_{(0)}{}^y + \hat{h}_{P(0)y}) \text{ at } \xi = 0. \tag{2.19b}$$

If a Taylor series expansion around $x = 0$ is used for $\bar{\psi}$, (2.10) and (2.15) may be substituted into the matching conditions (2.9c,d) and terms of the same order may be collected to yield (Allen, 1976b):

$$\bar{\psi}_{0y}(x = 0) = 0, \tag{2.20a}$$

$$\bar{\psi}_{0xt}(x = 0) = \psi_{0\xi t}(\xi = 1), \tag{2.20b}$$

Assuming that a boundary condition for $\bar{\psi}_0$, similar to (2.20a), holds on the other boundaries of the interior region, the lowest order barotropic motion in the interior may be determined from (2.11), (2.20a), and that condition, and is uncoupled from the shelf motion.

The relations (2.12), (2.15b), and (2.16) are substituted for $\bar{h}$ and h in (2.9a,b) and a Taylor series expansion around $x = 0$ is utilized for $\bar{h}_P$ to yield the matching conditions for the perturbation interface, i.e.,

$$\bar{h}_B(x = \delta) = \hat{h}(\xi = 1), \tag{2.21a}$$

$$\bar{h}_{Px}(x = 0) + \bar{h}_{Bx}(x = \delta) = \delta^{-1}\hat{h}_\xi(\xi = 1). \tag{2.21b}$$

The two terms on the left-hand side of (2.21b) are retained with the anticipation that, over the total frequency range, either one may be important in balancing the right-hand side.

3. The free wave solutions

Before proceeding to the forced problem, it is useful to have an understanding of the unforced or free wave problem. The detailed solutions to (2.17a,b) for the free waves are discussed in Allen and Romea (1980) (henceforth denoted as AR), and only a brief summary will be presented here.

We adopt an f-plane analysis ($\beta = 0$, f = constant), and choose the exponential shelf profile of Buchwald and Adams (1968), i.e.,

$$H = \exp[(\xi - 1)/\delta_B]. \tag{3.1}$$

In this case, $H_\xi/H = \delta_B{}^{-1}$ is a constant. This depth profile, while still highly idealized, is not an unreasonable approximation to actual shelf slope topography.

The equation for the free waves may be written

$$(\psi_{0\xi}/H)_{\xi t} + (H_\xi/H^2)(f\psi_{0y} - \hat{h}_y) = 0, \tag{3.2a}$$

$$(\hat{h}_\xi/aH)_{\xi t} - \delta_K^{-2}(\hat{h}_t/H_1) - f(H_\xi/H^2)(f\psi_{0y} - \hat{h}_y) = 0, \tag{3.2b}$$

$$\psi_{0y} = 0,\ f\hat{h}_y + \hat{h}_{\xi t} = 0 \text{ at } \xi = 0, \tag{3.3a,b}$$

$$\psi_{0\xi t} = 0,\ \hat{h}_\xi + \delta_{RI}^{-1}\hat{h} = 0 \text{ at } \xi = 1. \tag{3.4a,b}$$

By multiplying (3.2a) and (3.2b) by, respectively, ψ_0 and $\hat{h}$, integrating the two equations over ξ from 0 to 1, assuming periodicity in y and integrating over a period in y, we obtain an equation for the total energy density:

$$\epsilon = \tfrac{1}{2}\left\{\int_0^1 [H^{-1}\psi_{0\xi}^2 + (af^2H)^{-1}\hat{h}_\xi^2 + (f^2\delta_R^2H_1)^{-1}\hat{h}^2]d\xi + [(\delta_R aHf^2)^{-1}\hat{h}^2]_{(1)}\right\}. \tag{3.5}$$

As a result of assumptions (2.5b), all of the coastal trapped waves in the present model are nondispersive. Accordingly, free wave solutions are sought in the form

$$(\psi_0,\hat{h}) = Re\{\exp[-i\omega(t + c^{-1}y)](\phi(\xi),g(\xi))\}, \tag{3.6}$$

where ω is the radian frequency, c is the phase velocity, and *Re* denotes the real part.

The equations and boundary conditions for the eigenfunctions (ϕ_n, g_n) with corresponding eigenvalues c_n are

$$\phi_{n\xi\xi} - \delta_B^{-1}\phi_{n\xi} + (\delta_B c_n)^{-1}(f\phi_n - g_n) = 0, \tag{3.7a}$$

$$g_{n\xi\xi} + a\delta_B^{-1}g_{n\xi} - \delta_R^{-2}g_n - a(\delta_B c_n)^{-1}f(f\phi_n - g_n) = 0, \tag{3.7b}$$

$$\phi_n = 0,\ g_{n\xi} + (f/c_n)g_n = 0 \text{ at } \xi = 0, \tag{3.8a,b}$$

$$\phi_{n\xi} = 0,\ g_{n\xi} + \delta_R^{-1}g_n = 0 \text{ at } \xi = 1. \tag{3.9a,b}$$

The orthogonality relation for the eigenfunctions is

$$f^{-1}\left\{\int_0^1 (\delta_B H)^{-1}(f\phi_n - g_n)(f\phi_m - g_m)d\xi + [(aH)^{-1}g_n g_m]_{(0)}\right\} = \delta_{mn}c_n\epsilon_n, \tag{3.10a}$$

where, from (3.5), the energy density for each mode is

$$\epsilon_n = \frac{1}{2}\left\{\int_0^1 [H^{-1}\phi_{n\xi}^2 + (af^2H)^{-1}g_{n\xi}^2 + (f^2\delta_R^2H_1)^{-1}g_n^2]d\xi + [(\delta_R aHf^2)^{-1}g_n^2]_{(1)}\right\}. \tag{3.10b}$$

The factor on the right-hand side of (3.10a) follows from multiplying (3.7a,b) for

(ϕ_n, g_n) by, respectively, ϕ_n and g_n, integrating over ξ from 0 to 1 and combining. The result is

$$c_n \epsilon_n = \kappa_n = \frac{1}{2} f^{-1} \left\{ \int_0^1 (\delta_B H)^{-1} (f\phi_n - g_n)^2 d\xi + [(aH)^{-1} g_n^2]_{(0)} \right\} . \quad (3.11)$$

We may rewrite (3.11) as

$$c_n^{-1} = \epsilon_n / \kappa_n . \quad (3.12)$$

Eq. (3.12) represents a variational formulation of (3.7) and (3.8) in the sense that the admissible functions (ϕ_0, g_0) which minimize the quotient ϵ_n/κ_n are eigenfunctions for the problem defined by (3.7) and (3.8), and the minimum value is the associated eigenvalue c_0^{-1}. If the orthogonality condition (3.10a) is imposed, the variational formulation results in an increasing sequence of values for c^{-1}, e.g., c_1^{-1} is the minimum of ϵ_n/κ_n among functions orthogonal to (ϕ_0, g_0). In addition,

$$\lim_{n \to \infty} c_n^{-1} = \infty , \quad (3.13)$$

and the eigenfunctions (ϕ_n, g_n) form a complete set (Courant and Hilbert, Vol. 1, pp. 412, 424-426). The result (3.13) was demonstrated explicitly in Appendix B of Allen (1975).

Similar variational principles are obtained by Clarke (1976) and Huthnance (1978) in connection with the eigenvalue problem for coastal trapped waves in a continuously stratified fluid. One additional consequence of (3.12) (also reported by Clarke and Huthnance) is that for monotonic H, the right-hand side of (3.12) is positive definite and all free waves propagate poleward (toward $-y$).

While (3.7b) and (3.9b) have non-constant coefficients, if we assume that

$$a_{(0)} = H_1 / H_{2(0)} << 1, \quad (3.14)$$

(3.7a,b), (3.8a,b), and (3.9a,b) may be solved by perturbation methods, as in AR. The eigenfunctions consist of an infinite set of "shelf wave" (SW) solutions (ϕ_n, g_n), $(n = 1,2, \ldots)$, and a single internal Kelvin wave (IKW) solution (ϕ_0, g_0). At mid-latitudes, $\delta_R << 1$, the SW modes are barotropic and have offshore structures which are essentially those found for barotropic continental shelf waves in an unstratified ocean. For $\delta_R >> 1$, the SW modes are "bottom trapped," i.e., all their motion is confined to the lower layer. The IKW mode is baroclinic and has an offshore structure and wave speed similar to that obtained for a flat bottom internal Kelvin wave. In this case, however, there is a barotropic contribution to the onshore velocities from ϕ_0.

The phase speed c_0 of the IKW mode is independent of f while the SW mode phase speeds depend on f. Estimates of c_0 and c_1 (the first SW mode) are calculated in Appendix B of AR for the Pacific coast of South America. For latitudes less than 5S, $c_0 >> c_1$, i.e., the IKW mode travels faster than the first SW mode, while for

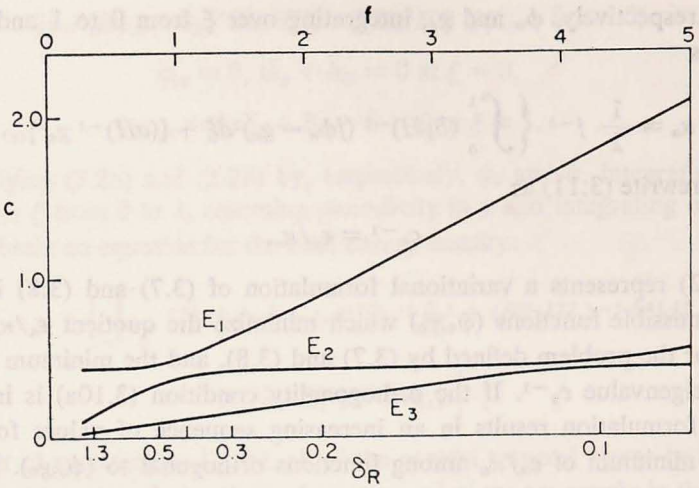

Figure 1. Variation of wave speeds as a function of δ_R for the 3 eigenfunctions E_1, E_2, and E_3, which, for $\delta_R < 0.43$, represent the internal Kelvin wave, the $n = 1$ and the $n = 2$ shelf waves, respectively. The values $a_{(0)} = 0.3$ and $\delta_B = 0.33$ have been utilized. Dimensionless f ($f = f'/f'_e$, where f'_e is the dimensional latitude for the interaction between the internal Kelvin wave and the $n = 1$ shelf wave) is plotted along the top axis. With dimensional values of shelf width $L_s = 90$ km and internal Kelvin wave phase speed $c'_0 = 100$ cm s^{-1}, $\delta_R = c'_0/(f'L_s)$ is plotted along the bottom axis, where $\delta_R = 0.43$ at the critical latitude $f' = f'_e$. Corresponding latitudes for $f = 1, 2, 3, 4, 5$ are 10°, 21°, 32°, 45°, and 63°, respectively.

mid-latitudes, $c_0 << c_1$, i.e., the first SW mode travels faster than the IKW mode. The two wave modes have the same phase speeds at a latitude of about 10S.

For parameter values where the wave speeds of the IKW mode and a SW mode are nearly equal, i.e., where $c_0 \cong c_n$, there is a coupling between the two types of wave modes. A plot of the phase speeds for the first three eigenfunctions as a function of δ_R is shown in Figure 1. As is indicated by the behavior of the wave speeds as a function of δ_R the mode which is originally an IKW becomes a first SW mode, and vice versa. At a larger value of δ_R, a similar behavior occurs for the IKW and second SW modes.

Note that, while the parameter δ_R varies strongly with latitude, it is also a function of shelf width, so it is possible, for example, for δ_R to be small at low latitudes for a very wide shelf.

4. Solutions via a cross-shelf modal analysis

Solutions to the shelf equations (2.17a,b), with the boundary conditions (2.19a,b), (2.20b), and (2.21a,b) may be obtained for a coastal wind stress with a general (y, t) structure by expanding the shelf variables in terms of the cross-shelf eigenfunctions of the unforced equations.

As in Section 3, an f-plane analysis is employed here and the assumptions in Section 2 (2.5a,b) are retained.

In a manner similar to (2.16) for h_0, we define

$$\psi_0 = \hat{\psi} + \bar{\psi}_{x(0)} \int_0^{\xi} H(\xi')d\xi'. \tag{4.1}$$

The last term in (4.1) represents the extension of the interior alongshore *velocity* at $x = \delta$ onto the shelf topography.[3]

With (4.1), the governing equations for the shelf variables (2.17a,b) are

$$(\hat{\psi}_{\xi\xi} - \delta_B^{-1}\hat{\psi}_\xi)_t - \delta_B^{-1}(\hat{h}_y - f\hat{\psi}_y) = \delta_B^{-1}F, \tag{4.2a}$$

$$(\hat{h}_{\xi\xi} + a\delta_B^{-1}\hat{h}_\xi - \delta_R^{-2}\hat{h})_t + fa\delta_B^{-1}(\hat{h}_y - f\hat{\psi}_y) = -a\delta_B^{-1}fF, \tag{4.2b}$$

where

$$F(\xi,y,t) = \tau_{(0)}{}^y + \bar{h}_{P(0)y} + f\bar{\psi}_{x(0)y} \int_0^{\xi} H(\xi')d\xi'. \tag{4.2c}$$

The boundary conditions at the coast are

$$\hat{\psi}_y = 0 \text{ at } \xi = 0, \tag{4.3a}$$

$$\hat{h}_{\xi t} + f\hat{h}_y = -fF \text{ at } \xi = 0. \tag{4.3b}$$

The solution to (2.14) (with $\beta = 0$) is:

$$\bar{h}_B = C_0(y,t)\exp(-x/\bar{\delta}_{RI}). \tag{4.4}$$

This solution may be used in (2.21a,b) to derive the boundary condition on $\hat{h}$ at $\xi = 1$. The boundary condition at $\xi = 1$ for $\hat{\psi}$ may be derived by introducing (4.1) into (2.20b). These conditions are

$$\hat{\psi}_{\xi t} = 0 \text{ at } \xi = 1, \tag{4.5a}$$

$$\hat{h}_\xi + \delta_{RI}{}^{-1}\hat{h} = 0 \text{ at } \xi = 1, \tag{4.5b}$$

where the term $\bar{h}_{Px(0)}$ is neglected relative to $\bar{\delta}_{RI}{}^{-1}\bar{h}_{Bx}$ and $\delta^{-1}\hat{h}_\xi$ in (2.21b), and where we use, from (2.21a),

$$\hat{h}(\xi = 1) = \bar{h}_B(x = \delta) = C_0\exp(-\delta_{RI}{}^{-1}). \tag{4.6}$$

This relation may be used to calculate C_0 and hence $\bar{h}_B$, after a solution is obtained for $\hat{h}$.

We now expand the shelf variables in terms of the eigenfunctions of the unforced problem, i.e.,

3. In Allen (1976b) the substitution $\psi_0 = \hat{\psi} + \xi\bar{\psi}_{x(0)}$ was used. This represents an extension of the interior alongshore *transport* onto the shelf. The definition (4.1) turns out to be more appropriate.

$$(\hat{\psi},\hat{h}) = \sum_{m=0}^{\infty} [\phi_m(\xi), g_m(\xi)] Y_m(y,t). \tag{4.7}$$

The series in (4.7) is summed over the single IKW pair (ϕ_0, g_0) and all the SW pairs (ϕ_n, g_n), ($n = 1,2, \ldots$). The expansions (4.7) for $\hat{\psi}$ and $\hat{h}$ are substituted into the shelf equations (4.2a,b) and the forced boundary condition at $\xi = 0$ (4.3b). If (4.2a,b) are multiplied by (ϕ_m, g_m) respectively, integrated with respect to ξ from 0 to 1, and are combined in a suitable manner with (4.3b) and the orthogonality relation (3.6), a forced first order wave equation is obtained for the (y,t) structure of each mode (Gill and Clarke, 1974; Clarke, 1977), i.e.,

$$c_m^{-1} Y_{mt} - Y_{my} = -T_m, \tag{4.8}$$

where

$$T_m(y,t) = f^{-1} \left\{ \int_0^1 (\delta_B H)^{-1} (f\phi_m - g_m) F d\xi \right.$$

$$\left. - [(aH)^{-1} g_m F]_{(0)} \right\}. \tag{4.9}$$

$T_m(y,t)$ contains two terms; one is integrated over the shelf and one is evaluated at the coast.

Two separate types of forcing contribute to F, i.e.,

$$F = \Phi + \hat{\tau}, \tag{4.10}$$

where

$$\Phi(\xi,y,t) = f\hat{\psi}_{xy(0)} \int_0^{\xi} H(\xi')d\xi', \tag{4.11a}$$

$$\hat{\tau}(y,t) = \tau_{(0)}{}^{y} + \hat{h}_{P(0)y}. \tag{4.11b}$$

The alongshore component of the wind stress at the coast and the baroclinic interior flow force motion on the shelf through the boundary condition at $\xi = 0$ and always appear together, while Φ, the effect of the interior barotropic flow, depends on ξ and vanishes at the coast ($\Phi_{(0)} = 0$; $F_{(0)} = \hat{\tau}$). For $\delta_R << 1$, $\hat{\tau}$ forces the IKW response mainly through the boundary term in (4.9), since g_0 decays rapidly from the coast and the contribution from the integral in (4.9) is small. The SW response arises predominantly from the integrated term in (4.9) which represents the cross-shelf bottom velocity u_2. For $\delta_R << 1$, an offshore barotropic flow interacting with a shelf-slope topography can force a SW response in this manner.

In order to examine the relative efficiency of excitation of the various modes by both $\tau_{(0)}{}^{y}$ and Φ we use (3.5), (3.10), (4.8) and (4.9) to calculate the total energy density ϵ_m of the lower modes. Approximate expressions for Y_m may be obtained for short time by solving (4.8) as an initial value problem with initial condition

$$Y_m(y,t=0) = 0. \tag{4.12}$$

For this case, the balance in (4.8) is $Y_{mt} \cong -c_m T_m$, and

$$\epsilon_m \cong \frac{1}{2}\left\{\int_0^1 [H^{-2}\phi_{m\xi}^2 + (f^2 aH)^{-1} g_{m\xi}^2 + \delta_R^{-2} H_1^{-1} g_m^2]d\xi \right.$$

$$\left. + [\delta_R^{-1}(afH)^{-1} g_m^2]_{(1)} \right\} T_m^2 c_m^2 t^2. \qquad (4.13)$$

Figures 2 and 3 show the energy density (divided by t^2) of the first several modes, forced by $\hat{\tau}$ and Φ, respectively, as a function of δ_R. As in Figure 1, we use the solutions derived in AR for $a_{(0)} << 1$. The mode which for $\delta_R << 1$ is an IKW is labelled E_1, while the mode which is a first mode SW is labelled E_2. The interaction (see Fig. 1) between E_1 and E_2 occurs at $\delta_R = 0.43$. For $\delta_R << 1$, E_1 is a first mode SW. E_2 interacts at $\delta_R = 0.11$ with E_3 (the second mode SW). Poleward of this interaction, E_3 is an IKW and E_2 is a second mode SW.

Without solving the interior problem for $h_{P(0)y}$ and $\tilde{\psi}_{x(0)}$, the relative importance of driving by $\hat{\tau}$ and Φ cannot be deduced, and we defer a discussion of this subject until Section 5. However, several points can be made from Figures 2 and 3, together with our understanding of the eigenfunctions discussed in Section 3.

Forcing by $\hat{\tau}$ for $\delta_R << 1$ results in an IKW response which is confined within δ_R of the coast and a set of barotropic SW modes which extend over the shelf. This implies that it is possible for interior baroclinic motions to drive barotropic motions on the shelf, although estimates using typical parameter values give $|\tau_{(0)}^y| >> |\tilde{h}_{P(0)y}|$. For $\delta_R >> 1$ the response to $\hat{\tau}$ consists of a baroclinic IKW mode which decays slowly into the interior and a set of "bottom trapped" SW modes. Hence, forcing by a surface wind stress or interior baroclinic motion yields a SW response on the shelf which is bottom intensified.

Figure 2 shows that, for $\delta_R >> 1$ and forcing by $\hat{\tau}$, E_1 (the IKW) is very efficiently excited, while E_2 (the bottom trapped first mode SW) is not very energetic. For latitudes less than 5°, the SW response is negligible. For $\delta_R << 1$, E_3 (the IKW) and E_1 (the first mode SW) are both excited, with the IKW more energetically forced than the SW. If kinetic energy density (not shown in Fig. 2) is considered instead of total energy density, the IKW mode, with $a_{(0)} = 0.3$, is less energetic than the first mode SW for $\delta_R > 0.15$, i.e., for latitudes >40°.

Note that, for a completely two-dimensional response, the dependence of h and ψ on y vanishes and (4.2a,b) uncouple. Forced solutions may be directly obtained and may be used in (4.13) to derive the total energy density which is also shown in Figure 2. The response will consist of an infinite sum of modes and the total energy of the response, of course, will be higher than that of the first two modes alone. Note, however, that the first two modes contain most of the energy.

The barotropic interior forcing excites an IKW response and a SW response on the shelf. Figure 3 shows that both the IKW and the SW responses are not forced

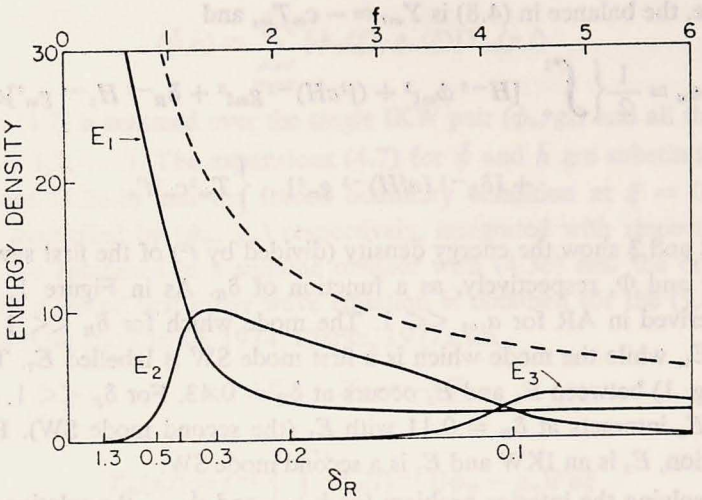

Figure 2. Energy density ϵ_m (4.13) divided by t^2 as a function of δ_R for the 3 eigenfunctions E_1, E_2, and E_3, forced by $\hat{\tau}$ ($\hat{\tau} = 1$). The dashed line represents the total energy density. The parameters used are the same as in Figure 1.

efficiently for $\delta_R >> 1$. For mid-latitudes, the IKW response (E_2) is not forced efficiently, while the first mode (barotropic) SW is relatively energetic.

Examples. It is useful to consider some simple solutions to (4.8). We focus only on driving by the alongshore component of the wind stress at the coast ($F = \tau_{(0)}{}^y(y,t)$), so that (4.8), (4.9) and (4.12) are

$$c_m{}^{-1} Y_{mt} - Y_{my} = -b_m \tau, \tag{4.14a}$$

$$b_m = f^{-1} \int_0^1 (\delta_B H)^{-1} (f\phi_m - g_m) d\xi - [(afH)^{-1} g_m]_{(0)}, \tag{4.14b}$$

$$\sum_{m=0}^{\infty} (f\phi_m - g_m) b_m = 1, \tag{4.14c}$$

$$Y_m (y, t = 0) = 0. \tag{4.14d}$$

In the following examples, we concentrate on the qualitative differences between the results at mid and low latitudes. (Examples at mid-latitude have been discussed by Allen [1976a].)

We first examine a simple impulsive wind stress with a limited alongshore extent, i.e.,

$$\tau(y,t) = \delta(t) T(y), \tag{4.15}$$

where, e.g.,

$$T(y) = \tau_0 \exp(-y^2/2). \tag{4.16}$$

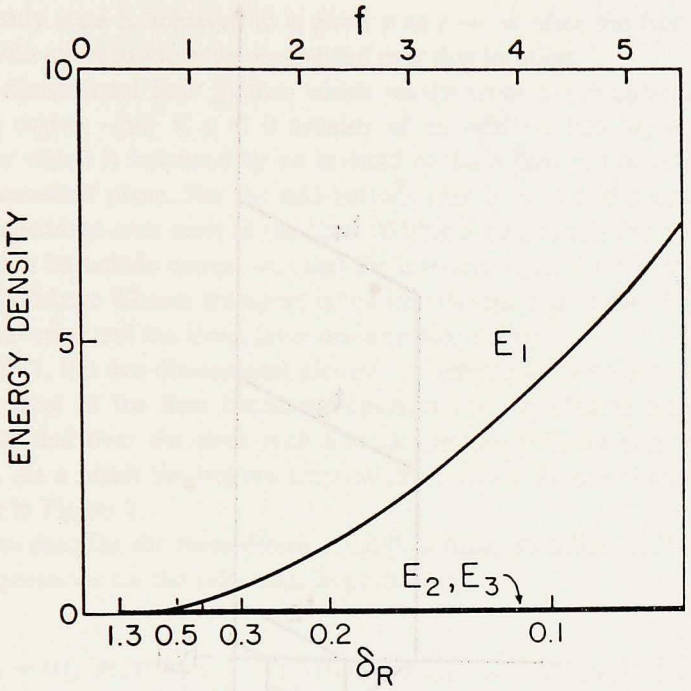

Figure 3. Energy density ϵ_m (4.13) divided by t^2 as a function of δ_R for the 3 eigenfunctions E_1, E_2, and E_3, forced by Φ, ($\tilde{\psi}_{xy(0)} = 1$). The parameters used are the same as in Figure 1.

The solution to (4.14a) with a wind stress given by (4.15) and (4.16) is

$$Y_m = -c_m b_m T(y - c_m t). \tag{4.17}$$

This solution corresponds to a response of limited extent propagating in the negative y direction (poleward) with speed c_m, for each mode. At low latitudes, the IKW response propagates relatively quickly away from the forcing region while the bottom trapped SW modes, whose phase speeds c_n are small compared with c_0, remain behind. This behavior can result in bottom intensified undercurrents over the continental slope.

We next consider an alongshore wind stress of the form

$$\tau(y,t) = H(t)T(y), \tag{4.18a}$$

where $H(t)$ is the Heaviside unit function. Here, for simplicity in illustrating the features of the solution (Allen, 1976a) we use the "top hat" function

$$T(y) = \begin{cases} 0 & 0 < y, \\ \tau_0 & -|y_0| < y < 0 \\ 0 & y < -|y_0| \end{cases} \tag{4.18b}$$

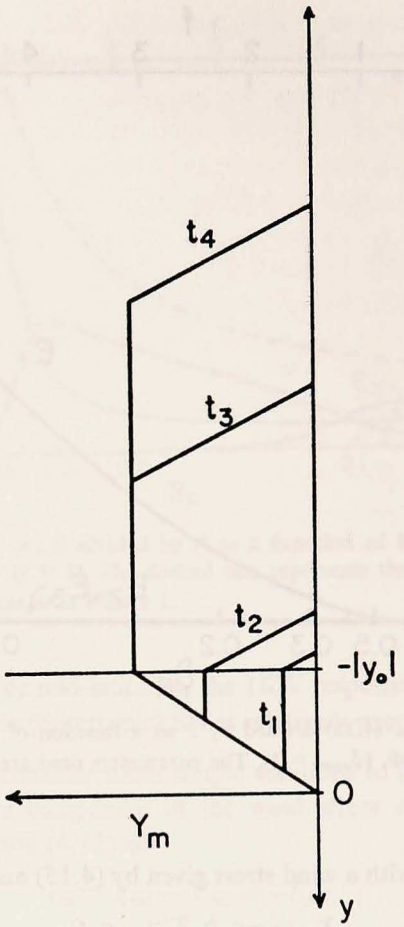

Figure 4. Y_m as a function of y for four values of t ($t_{i+1} > t_i$) [from Allen (1976a)].

The solution for Y_m as a function of y for various times is shown in Figure 4. This solution is obtained by the method of characteristics in Allen (1976a). For the purely baroclinic problem, Y_0 is the interface height at the coast, while for the purely barotropic problem Y_n gives the (y,t) structure in the expansion of the mass transport streamfunction in terms of the free shelf wave eigenfunctions.

The initial response, for $-|y_0| < y < -c_m t$, is time dependent and two-dimensional ($Y_{my} = 0$). The three-dimensional flow pattern develops as a free IKW front and a set of SW fronts are generated and propagate poleward (toward negative y). For $c_m t > |y_0|$, a region where Y_m is constant and where the alongshore velocity associated with a particular mode m is in steady geostrophic balance exists between the time dependent free wave front and the location of forcing, i.e., in $-c_m t < y <$

$-|y_0|$. A steady state is achieved at a given y as $t \to \infty$ after the free wave fronts associated with every mode have propagated past that location.

The two-dimensional flow pattern which results from the impulsive application of τ_0 in the region $-|y_0| < y < 0$ consists of an offshore flow u_E in the surface Ekman layer which is balanced by an inviscid onshore flow u_I toward the coast in the same cross-shelf plane. For the mid-latitude case $\delta_R << 1$, the onshore flow u_I is depth independent over most of the shelf. Within a distance δ_R from the coast the flow also has a baroclinic component and the interface rises. At $\xi = 0$, a mass flux equal to the offshore Ekman transport is fed into the surface Ekman layer from the upper layer interior and the lower layer onshore flux is zero.

For $\delta_R >> 1$, the two-dimensional picture is much the same except that the baroclinic component of the flow becomes important farther offshore and the flow is surface intensified over the shelf with a weak onshore velocity component in the lower layer. As a result the bottom trapped shelf waves are not efficiently excited, as is evident in Figure 2.

In order to describe the three-dimensional flow field, we utilize (4.7) in (2.18a-d) to obtain expressions for the velocities. In particular,

$$fu_1 = (H_1/H)a^{-1}\left\{\tau_0 + \sum_{m=0}^{\infty}[(af\phi_m + g_m)Y_{my} + f^{-1}g_{m\xi}Y_{mt}]\right\}, \tag{4.19a}$$

$$fu_2 = (H_1/H)\left\{-\tau_0 + \sum_{m=0}^{\infty}[(f\phi_m - g_m)Y_{my} - f^{-1}g_{m\xi}Y_{mt}]\right\}. \tag{4.19b}$$

The steady solution, with $Y_{mt} = 0$, $Y_{my} = b_m\tau_0$ and with (4.14c), is

$$fu_1 = (H_1/H)\,(1 + a)a^{-1}\sum_{m=0}^{\infty} f\phi_m b_m\tau_0, \tag{4.20a}$$

$$fu_2 = 0. \tag{4.20b}$$

When $Y_{mt} = 0$, we may write

$$Y_m = b_m\int_0^y \tau dy. \tag{4.21}$$

Utilization of (4.14c), (4.21), and (4.7) in (2.18d) yields the result that $v_2 = 0$. Hence for all δ_R the final steady solution over the slope has no motion in the lower layer.

The cross-shelf eigenfunctions obtained in AR and discussed in Section 3 of this paper may be used to examine the steady flow field in the upper layer. With $a_{(0)} << 1$, the IKW solution for g is

$$g_0 \cong \exp(-\xi/\delta_R), \tag{4.22}$$

while, for the SW modes

$$g_n = 0(a_{(0)}). \tag{4.23}$$

From (2.18), (4.7), (4.14), (4.22), and (4.23), u_1 and v_1 may be expressed as

$$fu_1 \cong \tau_0[1 - \exp(-\xi/\delta_R)] + 0(a), \tag{4.24}$$

$$fv_1 \cong \delta^{-1} \exp(-\xi/\delta_R) \int_0^y \tau dy + 0(a). \tag{4.25}$$

Eqs. (4.24) and (4.25) show that baroclinic processes bring u_1 to zero at $\xi = 0$ within a scale of δ_R, and that the final steady alongshore flow in the upper layer is confined to a region with an offshore scale of the Rossby radius (this result and the limiting behavior $u_2, v_2 \to 0$ was not pointed out in Allen [1976a]).

The flow pattern that develops at mid-latitudes is different from that at low latitudes and we will briefly discuss each case. The qualitative discussion given here can be easily verified using the approximate solution for the eigenfunctions given in AR for a "weak slope" and with the assumption $a_{(0)} << 1$.

For mid-latitudes, the Rossby radius is a fraction of the shelf width. The SW modes are barotropic and the first several modes ($c_n > c_0$) travel faster than the IKW mode while the remainder ($c_n < c_0$) travel slower. Fluid is drawn onshore in a region near each SW front and the region of onshore flow to the shelf-slope region propagates poleward with the SW phase speed. (The region of dominant onshore flow occurs in connection with the first mode SW and propagates poleward with the first mode SW phase speed.) The solution for increasing t, as the first several SW modes achieve a steady balance but before the IKW front has propagated away from the forcing region, consists of an equatorward barotropic alongshore current which connects the locations where fluid is drawn onto the slope to the region of forcing. The IKW front propagates into this barotropic current, leaving behind a steady baroclinic alongshore current which is positive in the upper layer and negative in the lower layer and which is confined within a baroclinic deformation radius of the coast. As the slower SW modes attain a steady state they adjust the velocities in the bottom layer to zero and concentrate the upper layer flow within a scale of δ_R.

At low latitudes, the IKW mode has a large offshore scale with respect to the shelf width and propagates poleward with a much faster speed than the SW modes which are bottom trapped. A schematic of the flow field for low latitudes is shown in Figure 5. When the IKW mode has propagated away from the forcing region, the onshore flow in the bottom layer turns poleward in a broad region within δ_R of the coast. The velocity in the bottom layer is poleward up to the location of an IKW front, where the density interface moves vertically upward (Allen, 1976a). The corresponding return flow in the top layer, from the location of the wave front to the region where the stress acts, is turned and fed horizontally to the coast, and, to-

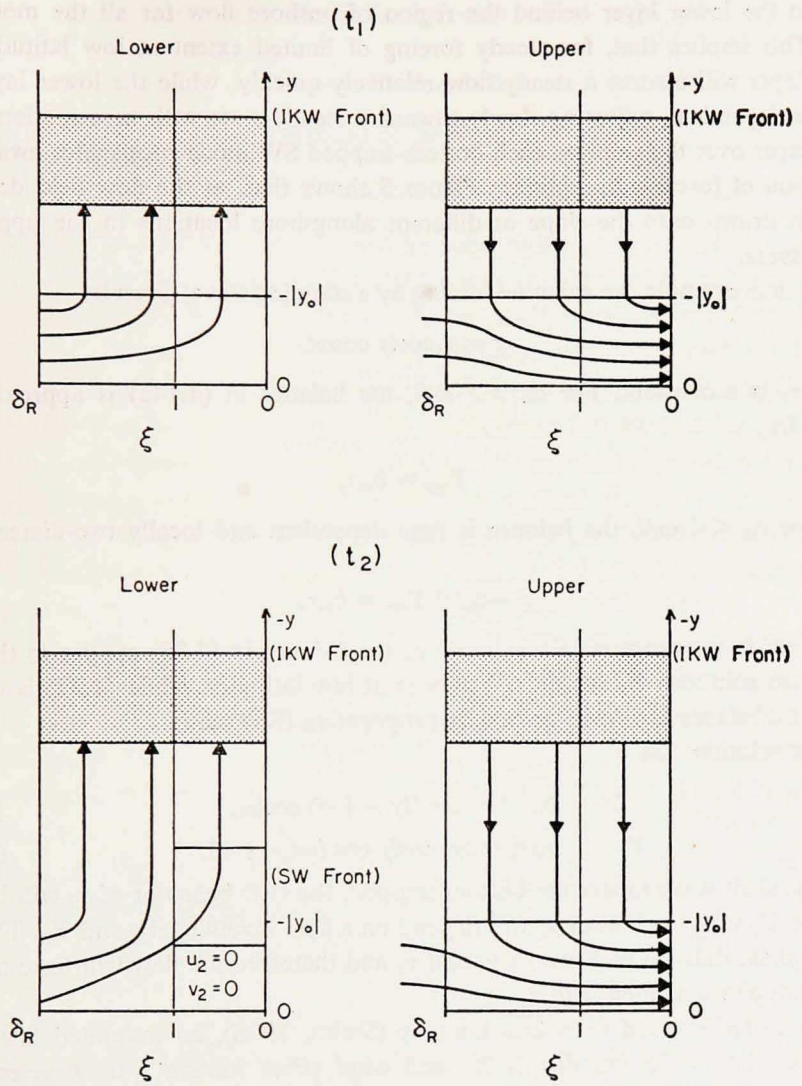

Figure 5. A schematic of the flow pattern that develops at low-latitudes in the upper and lower layers for a constant wind stress which is switched on at $t = 0$ in the region $-|y_0| < y < 0$. For simplicity, the effects of all the SW modes are represented by one SW front. Regions where the density interface moves vertically upward are shaded. The upper layer flow pattern does not include the offshore flow due to the surface Ekman layer.

gether with a component of the flow which comes directly onshore in the upper layer, is fed into the surface Ekman layer at $\xi = 0$. The SW modes are forced by the stress driven onshore flow in the lower layer and respond such that the location of the onshore flow to the slope in the lower layer propagates poleward. The velo-

cities in the lower layer behind the region of onshore flow for all the modes are zero. This implies that, for steady forcing of limited extent at low latitudes, the upper layer will assume a steady flow relatively quickly, while the lower layer will be time dependent, adjusting slowly toward a steady state with zero motion in the lower layer over the slope as each bottom-trapped SW mode propagates away from the region of forcing. In addition, Figure 5 shows that, as the flow field develops, water is drawn onto the slope at different alongshore locations in the upper and lower layers.

As a final example, we examine forcing by a standing wave, given by

$$\tau = \tau_0 \cos ly \cos \omega t, \tag{4.26}$$

where τ_0 is a constant. For $c_m >> \omega/l$, the balance in (4.14a) is approximately steady, i.e.,

$$Y_{my} = b_m \tau, \tag{4.27}$$

while for $c_m << \omega/l$, the balance is time dependent and locally two-dimensional, i.e.,

$$-c_m^{-1} Y_{mt} = b_m \tau. \tag{4.28}$$

For ω/l in the range $c_0 >> \omega/l >> c_n$ the balance in (4.28) applies to the time dependent solutions Y_n for the SW modes at low latitudes, while (4.27) is the approximate balance for the more rapidly propagating IKW mode.

These solutions are

$$Y_0 = b_0 l^{-1} \tau_0 \cos (ly - \tfrac{1}{2}\pi) \cos \omega t, \tag{4.29a}$$

$$Y_n = -b_n (c_n/\omega) \tau_0 \cos ly \cos (\omega t - \tfrac{1}{2}\pi). \tag{4.29b}$$

Since the shelf wave modes are bottom trapped, the (y,t) behavior of v_1 will be governed by Y_0 whereas that of v_2 will depend on a sum involving Y_0 and Y_n. This will lead to phase differences between v_1 and v_2 and therefore the flow will have a depth dependent phase relation with τ.

With an IKW speed $c_0 \cong 200$ km/day (Smith, 1978), an estimated first mode wave speed $c_1 \cong 25$ km/day (AR), and wind stress forcing with wavelength $\cong$ 1000 km, the solutions (4.29a,b) are valid for wind stress forcing with period in the range 5 days $< T <$ 40 days.

5. Sinusoidal forcing

We now consider solutions for the interior and shelf motion when the wind stress has a sinusoidal dependence on time and on the horizontal spatial coordinates, i.e.,

$$(\tau^x, \tau^y) = Re\{T_0 \exp[-i(\omega t - kx - ly)]\}, \tag{5.1}$$

so that the wind stress curl becomes

$$\tau_x{}^y - \tau_y{}^x = Re\{imT_0 \exp[-i(\omega t - kx - ly)]\}, \tag{5.2}$$

where

$$m = k - l,\ \omega > 0. \tag{5.3a,b}$$

We look for interior and shelf solutions of the form

$$(\tilde{\psi}_0, \tilde{h}_0, \psi_0, \hat{h}) = Re\{[\tilde{\phi}(x), \tilde{g}(x), \phi(\xi), \hat{g}(\xi)] \exp[-i(\omega t - ly)]\}. \tag{5.4}$$

Equations for $\tilde{\phi}$ and $\tilde{g}$ may be obtained by substituting (5.4) in (2.11), (2.13) and (2.14) while equations for the shelf variables may be obtained by utilizing (5.4) in (2.17a,b) (Appendix A). As in Section 4, the shelf equations are forced at the boundary $\xi = 0$ by $\tau_{(0)}{}^y$ and by interior baroclinic wind forced motions. In addition, interior wind forced barotropic motion $\tilde{\phi}$ drives a flow on the shelf through the boundary condition at $\xi = 1$ (A13c). Expressions for the interior motions are presented in Appendix A (A1-A4), and $\tilde{\phi}_{x(0)}$, the relevant expression for interior barotropic forcing at $\xi = 1$ is given by (A7). In general, $\tilde{\phi}_{x(0)}$ is complex and the shelf circulation due to $\tilde{\phi}$ will have components both in phase and out of phase with $\tau_{(0)}{}^y$. Examination of the forcing terms in (A12a,b) and (A13b) indicates that the response over the shelf due to $\tau_{(0)}{}^y$ is $\pi/2$ out of phase with the wind.

Figure 6 shows the absolute value of $\tilde{\phi}_{x(0)}$ scaled by T_0/ω for various k/l as a function of inverse frequency scaled as $\beta(2\omega\delta l)^{-1}$. Figure 7 shows the phase of $\tilde{\phi}_{x(0)}$. For $l >> k$ (alongshore traveling wind) the phase relation between components driven by $\tilde{\phi}_{x(0)}$ and $\tau_{(0)}{}^y$ changes considerably as a function of ω, with these components being $\pi/2$ out of phase for $\beta(2\omega\delta l)^{-1} << 1$ and in phase for $\beta(2\omega\delta l)^{-1} \cong 1$. For $k >> l$ (onshore traveling wind) the phase difference is $\cong \pi/2$. Therefore, motions on the shelf driven by $\tilde{\phi}$ and $\tau_{(0)}{}^y$ will exhibit a phase relation which is dependent on the frequency and wavenumbers of the wind.

a. Forced coastally trapped waves. In Appendix A it is shown that for forcing at moderate frequency (A5a,b) (e.g., $T' < 60$ days for oceanic parameters at 6° latitude off the west coast of South America) the interior baroclinic forcing term is negligible compared to T_0 (A15) and hence is neglected in the calculated examples below. Also, the interior barotropic forcing is given by the approximate form (A8a)

$$\tilde{\phi}_{x(0)} \cong T_0/\omega. \tag{5.5}$$

The validity of this approximation for forcing at moderate frequencies is also discussed in Appendix A.

With (A5a,b), the equations for the shelf variables are given by (A12a,b) and solutions which represent coastally trapped waves may be obtained by perturbation methods for $a_{(0)} << 1$ using an exponential slope topography (Appendix B). These solutions are presented in Figures 8-10 with $T_0 = 1$, where the figures show the contributions of forcing by the wind stress at $\xi = 0$ and by interior barotropic motions

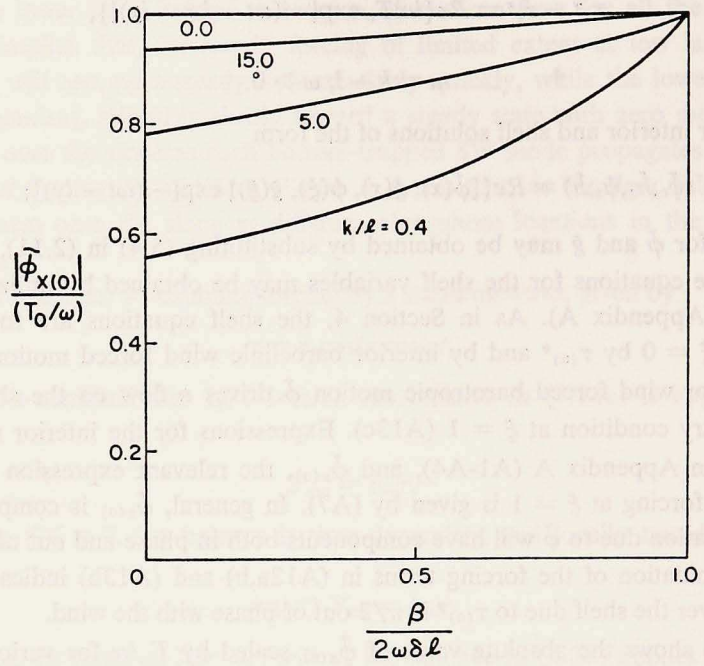

Figure 6. Scaled interior barotropic forcing $|\hat{\phi}_{x(0)}|/(T_0/\omega)$ as a function of scaled inverse frequency $\beta(2\omega\delta l)^{-1}$ for various values of k/l.

at $\xi = 1$. The parameters we vary are δ_B, δ_R, and l/ω. Figures 8 and 9 represent solutions for $l > 0$. We choose $a_{(0)} = 0.3$ (the results are relatively insensitive to the value of $a_{(0)}$ in the range $0.05 < a_{(0)} < 0.3$). As indicated above, the forcing in (A12a,b) and (A13b,c) appears as T_0/ω, if l/ω is regarded as a parameter. Accordingly, the velocities in Figures 8-10 have been rescaled with ω, i.e.,

$$V_i = v_i\omega, \; i = 1,2. \tag{5.6}$$

Note that, in comparing solutions at different latitudes (i.e., different δ_R), l/ω contains a factor of f_0, and l/ω corresponding to a wave with a certain period and wavelength will vary with f_0 (e.g., in Figs. 8a,b a wave with period $T' = 10$ days and wavelength $\lambda' = 1000$ km corresponds to $l/\omega \cong 16$ for $\delta_R = 0.05$ and $l/\omega \cong 0.4$ for $\delta_R = 2.0$).

Figures 8a and 8b show V_1 and V_2 on the shelf ($0 \leqslant \xi \leqslant 1$) for $\delta_R = 0.05$ and $\delta_R = 2.0$ respectively. The subscripts τ and Φ refer to forcing by $\tau_{(0)}{}^y$ and interior barotropic motions, respectively. The phase relation between V_Φ and τ may be obtained from Figure 7 with $\beta = 0$. Figure 8a is the mid-latitude case and, except on the inner shelf, the flow is barotropic. The highly baroclinic region near $\xi = 0$ is due to the forced internal Kelvin wave which decays rapidly away from the coast. The interior motion forces a non-negligible barotropic shelf response which is con-

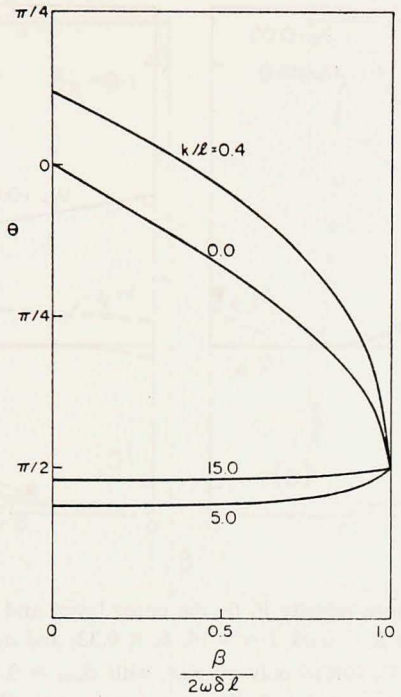

Figure 7. Phase difference θ between $\hat{\phi}_{x(0)}$ and $\tau_{(0)}{}^{y}$ as a function of $\beta(2\omega\delta l)^{-1}$ for various values of k/l.

fined to the outer slope. This behavior is evident in the approximate solutions (B10a,b) given in Appendix B for $\delta_R << 1$.

Figure 8b shows V_1 and V_2 for the low latitude case ($V_{1\tau}$ is rescaled for ease in plotting). These solutions are qualitatively very different from the mid-latitude response, due to the increased decay scale for baroclinic motions at low latitudes, and to the increased coupling between the equations (A12a,b) for the shelf variables. For low latitudes, the response over the entire shelf-slope region is highly baroclinic. V_1 is dominated by the forced internal Kelvin wave. This is evident in Figure 8b, where V_1 decays with $\exp(-\xi/\delta_R)$ with only a slight modification due to other terms. This behavior may be seen in the approximate solution (B11a,b) given in Appendix B for $\delta_R >> 1$, where the contribution to the alongshore velocity in the upper layer due to $\hat{\phi}_0$ is cancelled by the $0(a)$ correction to $\hat{g}$. This is equivalent to bottom trapping of the modal SW forced response at low latitudes. Similar qualitative behavior was obtained by Clarke (1976) with a step shelf topography. For $\delta_R >> 1$, $V_{2\Phi} \geqslant V_{2\tau}$ over the whole shelf region. Similar behavior is evident in the low latitude approximate solution (B11b), where $v_{2\tau}$ is $0(\delta_R)$ while $v_{2\Phi}$ is $0(1)$. Note also that $v_{2\tau}$ is relatively large near the shelf edge and decreases toward mid-shelf.

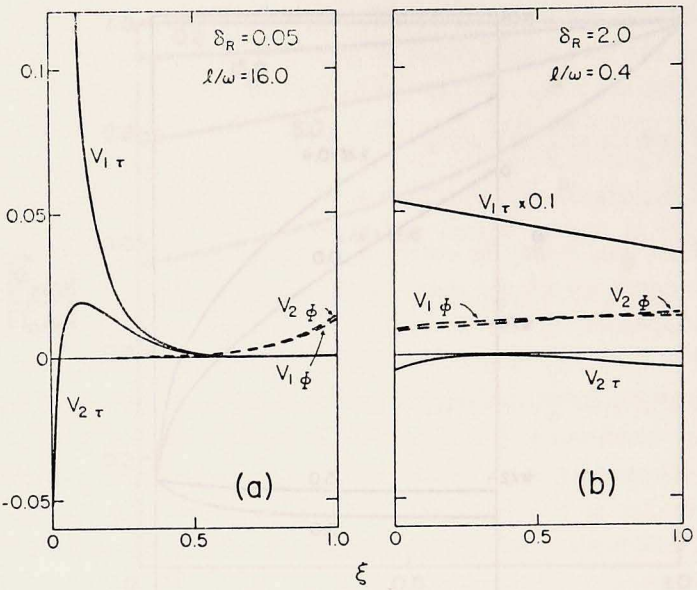

Figure 8. (a) Scaled alongshore velocity V_1 (in the upper layer) and V_2 (in the lower layer) over the shelf ($0 \leqslant \xi \leqslant 1$), for $\delta_R = 0.05$, $l/\omega = 16$, $\delta_B = 0.33$, and $a_{(0)} = 0.3$ ($V_i = v_i\omega$, $i = 1,2$). The solid line represents V_τ forced only by $\tau_{(0)}{}^y$, with $\hat{\phi}_{x(0)} = 0$. The dashed line represents V_Φ, forced only by $\hat{\phi}_{x(0)}$, with $\tau_{(0)}{}^y = 0$. $V_{1\tau}$ near $\xi = 0$ goes off scale ($V_{1(0)} = 0.51$). (b) V_1 and V_2 for $\delta_R = 2$, $l/\omega = 0.4$. $V_{1\tau}$ has been rescaled.

A dependence on latitude is also evident in Figures 9a-d where solutions have been plotted for $\delta_R << 1$ (9a,c) and $\delta_R >> 1$ (9b,d) for various ω/l. $V_{1\tau}$ decays away from $\xi = 0$ with $\exp(-\xi/\delta_R)$ in all cases. For $\delta_R = 0.1$, the decay is rapid, and the response is confined to the near-shore region. As δ_R becomes larger, the baroclinic decay scale increases, and the response extends across the entire shelf-slope region into the interior.

Figures 9b,d illustrate the growing importance of $V_{2\Phi}$ with respect to $V_{2\tau}$ as δ_R increases. Near $\xi = 1$, $V_{2\Phi}$ dominates for all δ_R. For $\delta_R << 1$, the wind forced motion is the dominant response for $\xi < 0.5$. For $\delta_R = 2.0$, $|V_{2\Phi}| > |V_{2\tau}|$ over the entire shelf-slope region.

We may examine the behavior of the exponential slope solutions given in Appendix B as a function of ω, keeping in mind the conditions (A5a,b) required to preserve their validity. In particular, for $\gamma^2 \cong l(\omega\delta_B)^{-1} >> 1$, $\gamma >> \delta_R{}^{-1}$, approximate solutions for the shelf velocities with low frequency forcing are given in Appendix B (B12a-c). The contribution to v_1 due to $\hat{\phi}$ is cancelled by part of the $0(a)$ correction to $\hat{g}$, which is equivalent to bottom trapping of the modal SW solutions when their cross-shelf scale is much less than the Rossby radius. The contribution to v_2 due to $\hat{g}_0$ is cancelled by part of $\hat{\phi}$, which implies that the IKW response be-

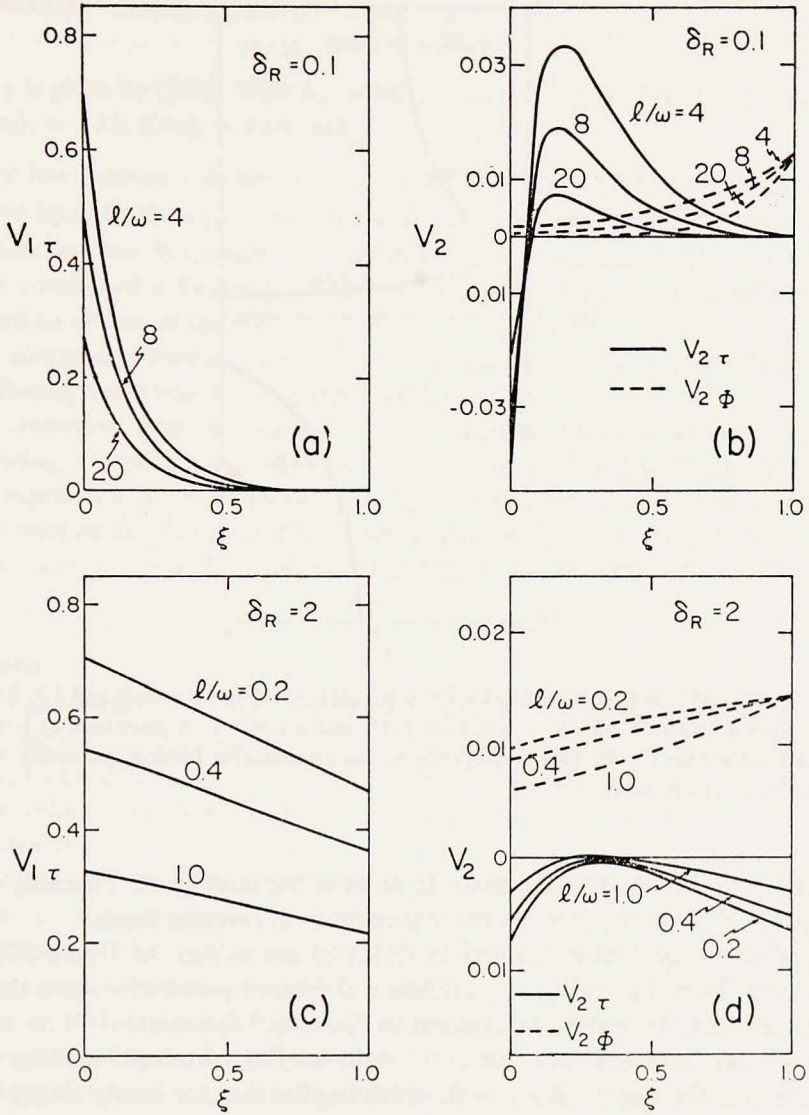

Figure 9. (a) $V_{1\tau}$; $\delta_R = 0.1$, (b) $V_{2\tau}$ and $V_{2\Phi}$; $\delta_R = 0.1$, (c) $V_{1\tau}$; $\delta_R = 2$, (d) $V_{2\tau}$ and $V_{2\Phi}$; $\delta_R = 2$, for various values of l/ω, with $\delta_B = 0.33$ and $a_{(0)} = 0.3$. $V_{1\Phi} << V_{1\tau}$ in both cases (a) and (c) and $V_{1\Phi}$ has not been plotted.

comes surface trapped for forcing at low frequency. v_1 is due entirely to the IKW response with offshore Rossby radius scale and $v_{2\tau}$ and $v_{2\Phi}$ are confined within boundary layers of width $\gamma^{-1}(<<\delta_R)$ and decay rapidly away from $\xi = 0$ and $\xi = 1$, respectively. Wind forced and interior barotropic motions penetrate less

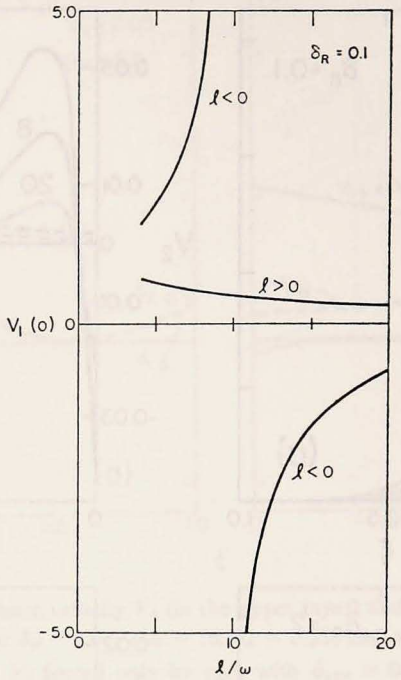

Figure 10. $V_{1\tau(0)}$ ($V_{1\tau}$ at $\xi = 0$) vs. l/ω for $l < 0$ (forcing traveling poleward) and $l > 0$ (forcing traveling equatorward), with $\delta_R = 0.1$, $\delta_B = 0.33$, and $a_{(0)} = 0.1$. A resonance at $|l/\omega| = 10$ occurs for the case $l < 0$. This corresponds to the atmospheric forcing resonating with the free internal Kelvin wave.

effectively onto the shelf in the lower layer as ω becomes small, reflecting the reluctance of low frequency motions to cross contours of constant depth.

Several of the qualitative features of (B12a-c) are evident in Figure 9b,d. For both $\delta_R >> 1$ and $\delta_R << 1$, $V_{2\Phi}$ exhibits a decreased penetration onto the shelf, and becomes more important with respect to $V_{2\tau}$, as ω/l decreases.

It is evident from (B12a-c) that as $\omega \to 0$, interior barotropic motions do not penetrate onto the slope and $v_{2\tau} \to 0$, which implies that for nearly steady forcing there is no motion in the lower layer. This corresponds to the limiting steady solution as $t \to \infty$ for "top hat" forcing (4.18), given in the modal analysis of Section 4.

The case $l < 0$ is more difficult to interpret due to the fact that the wind forcing can resonate with the free wave solutions. Figure 10 is a plot of $V_1(0)$ for $l > 0$ and $l < 0$ as a function of $l/\omega(\delta_R = 0.1)$, and clearly shows the resonance with the free internal Kelvin wave mode for $l/\omega = \delta_R^{-1} = 10$. There is a π phase shift as l/ω passes through the resonance.

In addition to the above resonance, free barotropic continental shelf waves over an exponential shelf will resonate with the wind forcing ($l < 0$) when γ satisfies (see

Appendix B)

$$\tan\gamma = -2\delta_B\gamma \tag{5.7}$$

where γ is given by (B5e). With $\delta_B = 0.33$, $a = 0.1$, the first three resonance points are $(l/\omega)_1 \cong 2.33$, $(l/\omega)_2 \cong 9.04$, and $(l/\omega)_3 \cong 22.09$.

b. Very low frequency behavior. The cases (A6a,b) and (A10a) where $\tilde{g}_I$ and $\tilde{g}_B$ are given by (A6c,d) respectively, and where $\tilde{\phi}_{x(0)}$ is given by (A10b) correspond to forcing at very low frequency ($T' > 60$ days). The approximate 0(1) motion in the interior consists of a Sverdrup balance in the upper layer which extends onto the shelf and no motion in the lower layer.

The alongshore coastal wind stress and interior baroclinic motions force an internal Rossby wave which propagates into the interior (Anderson and Gill, 1975).

The transition from a coastally trapped internal Kelvin wave to a westward propagating internal Rossby wave as the forcing frequency is lowered may be seen in the expression for R in (A4b). For $\delta_R{}^{-2} > (\frac{1}{2}\beta/\omega)^2$, the solution is coastally trapped with an oscillatory character. As $(\frac{1}{2}\beta/\omega)^2 \to \delta_R{}^{-2}$ the trapping scale grows, until $(\frac{1}{2}\beta/\omega)^2 \geqslant \delta_R{}^{-2}$ and the solution is no longer coastally trapped.

6. Summary

The main question we pose in the introduction is: what is the response on a continental shelf and slope to direct wind stress forcing and to forcing by interior motions, and how does this response vary with latitude? The simple theory presented here provides some answers to this question, and gives some insight for further observational and theoretical work.

In Section 2, it is shown that motions in the shelf-slope region are coupled to those in the interior ocean. The cross-shelf modal analysis of Section 4 clearly shows forcing of shelf circulations by interior barotropic and baroclinic flow. The modal solutions of Section 4 exhibit a dependence of the cross-shelf and vertical structure on latitude. At mid-latitudes, the barotropic (shelf wave) response extends over the shelf, while the baroclinic (internal Kelvin wave) response is confined to a region of width $\delta_R << 1$ near the coast. At low latitudes, the response is highly baroclinic over the entire shelf, reflecting the relatively large size of the baroclinic boundary layer. The shelf wave response is bottom intensified for low latitudes. This depth dependence, coupled with the fact that, for low latitudes, the internal Kelvin wave speed is larger than the $n = 1$ shelf wave speed, yields a different qualitative time dependent response to wind stress forcing than that obtained for mid-latitudes. With a constant wind stress forcing which is switched on at $t = 0$ and which has a limited extent in y (i.e., a "top hat" function), the upper layer assumes a steady flow relatively quickly with an offshore scale given by δ_R, while the lower layer remains time dependent, adjusting slowly toward a steady state of no motion.

Using the modal solutions of Section 4 and the energy density of each forced mode, we obtain an understanding of the relative efficiency of energy transfer into each mode. At low latitudes, $\tau_{(0)}{}^{y}$, the alongshore wind stress at the coast, forces a very energetic internal Kelvin wave, but is inefficient in forcing shelf waves. For driving by $\tau_{(0)}{}^{y}$ at mid-latitudes, the IKW and $n = 1$ SW modes have energy densities of the same order. However, the kinetic energy of the $n = 1$ SW mode is greater than that of the IKW mode at mid-latitudes. Interior barotropic motions do not efficiently excite the IKW or the SW modes at low latitudes. The $n = 1$ SW mode is efficiently excited, however, for mid-latitude offshore barotropic forcing.

A simple solution obtained with forcing by a traveling wave wind disturbance enables us to compare the relative effects of forcing by $\tau_{(0)}{}^{y}$ and by $\phi_{x(0)}$, offshore generated barotropic motions. With the assumptions of the present model, interior baroclinic motions are unimportant except for very low frequency driving.

Coastal wind stress forcing is an important effect for all latitudes. For mid-latitudes, interior driving mechanisms force motions on the shelf and slope which, for $\xi > 0.5$, are as large or larger than the coastal wind stress forced motion. The mid-latitude forced response over most of the inner shelf and slope ($\xi < 0.5$) is predominantly due to the local alongshore wind stress. However, the effect of interior forcing on the velocity in the *lower layer* grows with respect to the direct wind forced effect as δ_R becomes larger, and the low latitude forced response to interior barotropic motions $v_{2\Phi}$ can be comparable to or greater than the wind forced response $v_{2\tau}$.

For low frequency driving [$\frac{1}{2}\delta_{RI}\,\beta << \omega << |l|/\delta_B$, (20 days $< T' <$ 60 days at 6° latitude)], interior motions penetrate less effectively onto the shelf, reflecting the topographic constraint on low frequency circulations. The coastal wind forced response is also inhibited from crossing contours of constant depth, so that, for low frequency driving, the circulation over the outer shelf and slope is controlled predominantly by the interaction of the interior flow with the shelf. In cases where V_τ is concentrated near the coast and V_Φ is concentrated near the outer shelf, cross-shelf phase shifts of $\pi/2$ are predicted for driving by a wind which is traveling predominantly in the alongshore direction. In the general case, predicted cross shelf phase lags may be estimated using Figure 7. For forcing at very low frequency [$\omega << \frac{1}{2}\,\delta_{RI}\,\beta$, ($T' >$ 60 days at 6° latitude)], an interior Sverdrup flow in the upper layer extends onto the shelf and represents the dominant shelf response. Wave motions on the shelf are not coastally trapped, but propagate into the interior in the form of westward traveling long internal Rossby waves.

Finally, we point out that the ability of interior motion to contribute significantly to shelf-slope circulation is limited for this model by assumptions of a linear interior ocean driven locally by a wind stress curl. Strong nonlinear offshore baroclinic currents, for example, might drive appreciable baroclinic shelf motion at low latitudes. This problem remains to be investigated.

Acknowledgments. This research was supported by the Oceanography Section, National Science Foundation, under Grants DES 7515202, OCE-7826820 and OCE-8024116 and also by the Coastal Upwelling Ecosystems Analysis program (CUEA) of the Office of the International Decade of Ocean Exploration (IDOE) of the National Science Foundation under Grants OCE-7803382 and OCE-7803380.

APPENDIX A

Sinusoidal forcing

a. Interior solutions. With a wind stress given by (5.1), we seek interior solutions given by (5.4), and, in a manner similar to the representation for $\hat{h}$ in (2.12), we define

$$\hat{g}(x) = \hat{g}_P + \hat{g}_B. \tag{A1}$$

The solutions to (2.11), (2.13), and (2.14) for $\hat{\phi}$, $\hat{g}_P$ and $\hat{g}_B$, subject to (2.20a) and (2.21b) and appropriate for an eastern boundary, are

$$\hat{\phi} = -mT_0[\omega(k^2 + l^2) - (k\beta/\delta)]^{-1}\,[\exp(ikx) - \exp(Q_- x)], \tag{A2a}$$

$$Q_\pm = (i\beta/2\omega\delta) \pm [l^2 - (\beta/2\omega\delta)^2]^{1/2}, \tag{A2b}$$

$$\hat{g}_P = fmT_0[k\beta - \omega\delta\bar{\delta}_{RI}^{-2}]^{-1} \exp(ikx), \tag{A3}$$

$$\hat{g}_B = C_0 \exp(Rx), \tag{A4a}$$

$$R = (i\beta/2\omega\delta) - [\bar{\delta}_{RI}^{-2} - (\beta/2\omega\delta)^2]^{1/2}, \tag{A4b}$$

where assumption (2.5a) has been used in (5.7) and where the constant C_0 in (A4a) may be determined from (2.21a) after a solution for $\hat{h}$ on the shelf is obtained.

For

$$\omega >> k\beta\delta_{RI}^2\,\delta,\ \omega >> \frac{1}{2}\,\delta_{RI}\,\beta, \tag{A5a,b}$$

applied to (A3) and (A4) respectively, we obtain

$$\hat{g}_P \sim -fmT_0(\delta_{RI}^2\delta/\omega)\exp(ikx),\ \hat{g}_B \sim C_0\exp(-x/\bar{\delta}_{RI}). \tag{A5c,d}$$

Eq. (A5d) in the interior extension of a coastal trapped internal Kelvin wave. This case is investigated in Section 5a. Note that in general (A5b) implies (A5a) since $\bar{\delta}_{RI}\,k << 1$. Condition (A5a) corresponds to forcing at wavenumbers and frequencies above the cutoff for long internal Rossby waves.

For very low frequency forcing, i.e., for

$$\omega << k\beta\delta_{RI}^2\,\delta,\ \omega << \frac{1}{2}\,\delta_{RI}\,\beta, \tag{A6a,b}$$

we obtain

$$\hat{g}_P \sim fm(T_0/k\beta)\exp(ikx),\ \hat{g}_B \sim C_0\exp(i\omega\delta x/\beta\bar{\delta}_{RI}^2), \tag{A6c,d}$$

and the interior solution takes the form of an interior Sverdrup flow (A6c) and a westward propagating internal Rossby wave (A6d). This case is briefly discussed in Section 5b.

The relevant expression (2.20b) for the forcing at $\xi = 1$ by the interior barotropic motion is

$$\hat{\phi}_{x(0)} = im(T_0/\omega)\,(k + iQ_+)^{-1}. \tag{A7}$$

In general $\hat{\phi}_{x(0)}$ is complex and the forced shelf circulation will have components both in phase and out of phase with the wind stress driving. For the purposes of calculating specific solutions in Section 5a for the shelf velocities, we employ the approximate expression

$$\phi_{x(0)} \cong T_0/\omega, \tag{A8a}$$

obtained with the conditions

$$l^2 >> (\beta/2\omega\delta)^2,\ |k| \to 0. \tag{A8b,c}$$

The condition (A8b) is restrictive, implying the period $T' < 20$ days. However, for $l^2 \geqslant (\beta/2\omega\delta)^2$, with $|k| \to 0$,

$$|\phi_{x(0)}|^2 \sim (T_0/\omega)^2, \tag{A8d}$$

i.e., $\phi_{x(0)}$ has the same magnitude for the more general case (see Fig. 6 with $k/l = 0$).

The limit

$$l^2 \geqslant (\beta/2\omega\delta)^2,\ k >> l, \tag{A9a,b}$$

yields

$$\phi_{x(0)} \sim -i\, T_0/\omega. \tag{A9c}$$

and the response, while of the same magnitude as $\phi_{x(0)}$ obtained in the limit (A8b,c), is out of phase with the wind stress by a factor of $\pi/2$. This behavior is evident in Figures 6 and 7 with $k/l = 15.0$.

Condition (A8c) corresponds to a wind stress with x wavenumber $k = 0$, traveling along the coast. For $l < 0$ (equatorward traveling disturbance), $\phi_{x(0)} < 0$. For $l > 0$, $\phi_{x(0)} > 0$. Condition (A9b) corresponds to a wind stress traveling in the onshore-offshore direction. For both $k > 0$ and $k < 0$, $\phi_{x(0)} < 0$.

We also note that $\phi_{x(0)}$ is independent of ω for small ω, i.e., the condition

$$(|l|, |k|) << \beta/2\omega\delta \tag{A10}$$

yields

$$\phi_{x(0)} \sim im(T_0\delta/\beta), \tag{A11}$$

corresponding to a Sverdrup balance in the interior.

b. Shelf equations. We restrict our attention to cases where (A5a,b) are satisfied and use (A5c,d) for $\tilde{g}_P$ and $\tilde{g}_B$. For oceanic parameters at 6° latitude off the west coast of South America (e.g., $\delta_R' \cong 100$ km, $\beta' \cong 2.3 \times 10^{-13}$ cm $^{-1}$ sec^{-1}), (A5a,b) are satisfied for periods $T' < 60$ days.

We seek a forced response on the shelf of the form (5.4). The equations for the shelf variables, obtained by utilizing (5.4) in (2.17a,b) are

$$\phi_{\xi\xi} - \delta_B^{-1}\phi_\xi - l(\omega\delta_B)^{-1}(f\phi - \hat{g}) = i\hat{T}_0(\omega\delta_B)^{-1}, \tag{A12a}$$

$$\hat{g}_{\xi\xi} + a\delta_B^{-1}\hat{g}_\xi - \delta_R^{-2}\hat{g} + afl(\omega\delta_B)^{-1}(f\phi - \hat{g}) = -iaf\hat{T}_0(\omega\delta_B)^{-1}, \tag{A12b}$$

where

$$\hat{T}_0 = T_0 + il\tilde{g}_{P(0)}. \tag{A12c}$$

As in Section 4, the shelf equations are forced by the alongshore component of the wind stress at the coast and by the interior baroclinic motion.

With (5.4), the boundary conditions (2.19a,b), (2.20b), and (2.21a,b) are

$$\phi = 0,\quad f(l/\omega)\hat{g} - \hat{g}_\xi = if\,\hat{T}_0/\omega,\quad \text{at } \xi = 0, \tag{A13a,b}$$

$$\phi_\xi = \phi_{x(0)},\quad \text{at } \xi = 1, \tag{A13c}$$

$$\hat{g} = \tilde{g}_{B(\delta)},\quad \tilde{g}_{Px(0)} + \tilde{g}_{Bx(\delta)} = \delta^{-1}\hat{g}_\xi,\quad \text{at } \xi = 1. \tag{A14a,b}$$

With (A5a,b), except very near the equator, the interior baroclinic forced response is rela-

tively small. This is reflected in the ratio of the interior forcing term $il\bar{g}_{P(0)}$ and the coastal wind stress term T_0, which appear in the forcing $\hat{T}$; i.e.,

$$il\bar{g}_{P(0)}/T_0 \sim (ml/\omega)\, f\delta\, \delta_R{}^2 i, \tag{A15}$$

which is 0(δ) and therefore small. Accordingly, with (A5a,b) we employ the approximation

$$\hat{T} \cong T_0. \tag{A16}$$

Note that with (A6)

$$il\bar{g}_{P(0)}/T_0 \sim mlf(k\beta)^{-1} i, \tag{A17}$$

which is 0(1) in general, indicating that for forcing at very low frequencies baroclinic interior motions may be as important as the alongshore coastal wind stress.

APPENDIX B

Exponential slope

Analytical results to (A12a,b) are obtainable if an exponential slope (Buchwald and Adams, 1968) is assumed:

$$H = \exp[(\xi - 1)/\delta_B]. \tag{B1}$$

In this case, $H_\xi/H = \delta_B{}^{-1}$ is a constant. This depth profile, while still highly idealized, is not an unreasonable approximation to actual shelf-slope topography.

We obtain approximate solutions under the assumption

$$a_{(0)} = H_1/H_{2(0)} << 1. \tag{B2a}$$

We utilize the expansion

$$a = a_{(0)} \exp(-\xi/\delta_B) + 0(a_{(0)}{}^2), \tag{B2b}$$

so that (A12a,b) may be written to $0(a_{(0)}{}^2)$ in the form

$$\hat{\phi}_{\xi\xi} - \delta_B{}^{-1}\hat{\phi}_\xi - (l/\omega\delta_B)\,(f\hat{\phi} - \hat{g}) = 0, \tag{B3a}$$

$$\hat{g}_{\xi\xi} - \delta_R{}^{-2}\hat{g} = [a_{(0)}\exp(-\xi/\delta_B)]\,[-(fl/\omega\delta_B)\,(f\hat{\phi} - \hat{g}) - \delta_B{}^{-1}\hat{g}_\xi + \delta_R{}^{-2}\hat{g}], \tag{B3b}$$

where we define

$$\hat{\phi} = \phi + iT_0/l. \tag{B3c}$$

For simplicity, we adopt an f-plane analysis ($f = 1$) here, and assumptions (A5a,b).

The boundary conditions are

$$\hat{\phi} = iT_0/l, \quad \hat{g} - (\omega/l)\hat{g}_\xi = iT_0/l, \quad \text{at } \xi = 0, \tag{B4a,b}$$

$$\hat{\phi}_\xi = \hat{\phi}_{s(0)}, \quad \hat{g} = C_0, \quad \hat{g}_\xi + \delta_{RI}{}^{-1}\hat{g} = 0, \quad \text{at } \xi = 1, \tag{B4c,d,e}$$

where $\hat{\phi}_{s(0)}$ is given by (A8a) and C_0 is the coefficient from (A5d).

With (B2a), (B3a,b) are weakly coupled and may be solved, subject to (B4a-e), by perturbation methods. We solve (B3a) for $\hat{\phi}$ only, subject to (B4a,c), to obtain a first order approximation, $\hat{\phi}_0$. Similarly, we solve (B3b) for $\hat{g}$ only, subject to (B4b,e) to obtain a first order approximation, $\hat{g}_0$.

These are

$$\hat{g}_0 = K_0 \exp(-\xi/\delta_R), \tag{B5a}$$

$$\hat{\phi}_0 = \exp(\xi/2\delta_B)\,(D_0 \sinh\gamma\xi + iT_0 l^{-1}\cosh\gamma\xi), \tag{B5b}$$

where

$$K_0 = i(T_0/l)\,[1 + (\omega/l\,\delta_R)]^{-1}, \tag{B5c}$$

$$D_0 = \left[-i(T_0/l)\left(\frac{1}{2}\,\delta_B^{-1}\cosh\gamma + \gamma\sinh\gamma\right) + \hat{\phi}_{*(0)} \exp\left(\frac{1}{2}\,\delta_B\right)\right] \Big/ \left(\frac{1}{2}\,\delta_B^{-1}\sinh\gamma + \gamma\cosh\gamma\right), \tag{B5d}$$

$$\gamma^2 = (l/\omega)\delta_B^{-1} + (2\delta_B)^{-2}. \tag{B5e}$$

These solutions are written for $l > 0$.

We substitute $\hat{g}_0$ into (B3a) to obtain a 0(1) correction $\hat{\phi}_1$. The $0(a_{(0)})$ correction to $\hat{g}$, $a_{(0)}\hat{g}_1$, is obtained by substituting $\hat{\phi}_0$, $\hat{g}_0$, and $\hat{\phi}_1$ into (B3b). Finally, we utilize $a_{(0)}\hat{g}_1$ in (B3a) to obtain the $0(a)$ correction $a_{(0)}\hat{\phi}_2$ to $\hat{\phi}$. The corrections satisfy homogeneous boundary conditions at $\xi = 0$ and $\xi = 1$. Additional corrections are $0(a_{(0)}^2)$ so that the approximate solutions are

$$\hat{\phi} = \hat{\phi}_0 + \hat{\phi}_1 + a_{(0)}\hat{\phi}_2 + 0(a_{(0)}^2), \tag{B6a}$$

$$\hat{g} = \hat{g}_0 + a_{(0)}\hat{g}_1 + 0(a_{(0)}^2). \tag{B6b}$$

The corrections may be obtained in a straightforward manner but their algebraic form is complicated and they are omitted here.

This perturbation procedure was verified by comparison with expansions for $a_{(0)} << 1$ of exact solutions which may be obtained in the weak slope limit $\delta_B >> 1$.

The coefficient K_0 possesses a singularity for $\omega/l\ \delta_R = -1$ (see B6a), while D_0 is unbounded for

$$\tanh\gamma = -2\delta_B\gamma. \tag{B7}$$

The first singularity corresponds to wind forcing at the resonant frequency for free internal Kelvin waves, and (B7) corresponds to the excitation of the free shelf wave modes. These resonances occur only for $l < 0$.

Substitution of (5.5) into (2.18c,d) yields the shelf velocities:

$$v_1 = -\,\delta H\, H_1^{-1}\, \hat{v}_1(\xi) \quad \exp[-i(\omega t - ly)], \tag{B8a}$$

$$v_2 = -\,\delta H\, H_1^{-1}\, \hat{v}_2(\xi) \quad \exp[-i(\omega t - ly)], \tag{B8b}$$

where

$$\hat{v}_1(\xi) = \hat{\phi}_\xi + a^{-1}\hat{g}_\xi, \tag{B9a}$$

$$\hat{v}_2(\xi) = \hat{\phi}_\xi - \hat{g}_\xi. \tag{B9b}$$

The solutions (B6a,b) simplify considerably if the limits $\delta_R << 1$ and $\delta_R >> 1$ are examined. These approximate solutions may be utilized in (B9a,b) to obtain approximate shelf velocities. For $\delta_R << 1$,

$$\hat{v}_1(\xi) \cong -iT_0(a\omega)^{-1} \exp(-\,\xi/\delta_R) + M(\xi), \tag{B10a}$$

$$\hat{v}_2(\xi) \cong iT_0\omega^{-1} \exp(-\,\xi/\delta_R + M(\xi), \tag{B10b}$$

where

$$M(\xi) = \exp(\xi/2\delta_B)\,\{D_0[(2\delta_B)^{-1}\sinh\gamma\xi + \gamma\cos\delta\xi] + iT_0 l^{-1}\,[(2\delta_B)^{-1}\cosh\gamma\xi + \gamma\sinh\gamma\xi]\}. \tag{B10c}$$

For $\delta_R >> 1$,

$$\hat{v}_1(\xi) \cong -iT_0(al)^{-1}\,\delta_R^{-1} \exp(-\,\xi/\delta_R), \tag{B11a}$$

$$\hat{v}_2(\xi) \cong [\hat{\phi}_{x(0)} + iT_0\,(l\,\delta_R)^{-1}] \exp[(\xi - 1)/2\delta_B]$$

$$\times [(2\delta_B)^{-1}\sinh\gamma\xi + \gamma\cosh\gamma\xi]/[(2\delta_B)^{-1}\sinh\gamma + \gamma\cosh\gamma]. \quad \text{(B11b)}$$

We may also examine the behavior of the solutions for low frequency, keeping in mind the conditions (A5a,b) required to preserve their validity. In particular, for $\gamma^2 \cong l(\omega\delta_B)^{-1} >> 1$, $\gamma >> \delta_R^{-1}$,

$$\hat{v}_1(\xi) \cong -iT_0(al)^{-1}\,\delta_R^{-1} \exp(-\delta/\delta_R), \quad \text{(B12a)}$$

$$\hat{v}_2(\xi) \cong iT_0 l^{-1} L_0 \exp(-\gamma\xi) + \hat{\phi}_{x(0)}\gamma^{-1} \exp[\gamma(\xi - 1)], \quad \text{(B12b)}$$

where

$$L_0 = \omega/(l\,\delta_R) + \gamma^{-2}[\delta_R^{-2} + (\delta_R\delta_B)^{-1}]. \quad \text{(B12c)}$$

REFERENCES

Allen, J. S. 1975. Coastal trapped waves in a stratified ocean. J. Phys. Oceanogr., *5*, 300–325.

—— 1976a. Some aspects of the forced wave response of stratified coastal regions. J. Phys. Oceanogr., *6*, 113–119.

—— 1976b. On forced, long continental shelf waves on an *f*-plane. J. Phys. Oceanogr., *6*, 426–431.

Allen, J. S. and R. D. Romea. 1980. On coastal trapped waves at low latitudes in a stratified ocean. J. Fluid Mech., *98*, 555–585.

Anderson, D. L. T. and A. E. Gill. 1975. Spin up of a stratified ocean, with applications to upwelling. Deep-Sea Res., *22*, 583–596.

Brink, K. H., J. S. Allen and R. L. Smith. 1978. A study of low frequency fluctuations near the Peru coast. J. Phys. Oceanogr., *8*, 1025–1041.

Buchwald, V. T. and J. K. Adams. 1968. The propagation of continental shelf waves. Proc. Roy. Soc. London, *A305*, 235–250.

Clarke, A. J. 1976. Coastal upwelling and coastally trapped long waves. Ph.D. thesis, Cambridge University, 178 pp.

—— 1977. Observational and numerical evidence for wind-forced coastal trapped long waves. J. Phys. Oceanogr., *7*, 231–247.

Courant, R. and D. Hilbert. 1953. Methods of mathematical physics. Interscience, New York, 561 pp.

Gill, A. E. and A. J. Clarke. 1974. Wind induced upwelling, coastal currents, and sea level changes. Deep-Sea Res., *21*, 325–345.

Gill, A. E. and E. H. Schumann. 1974. The generation of long shelf waves by the wind. J. Phys. Oceanogr., *4*, 83–90.

Huthnance, J. M. 1978. On coastal trapped waves: analysis and numerical calculation by inverse iteration. J. Phys. Oceanogr., *8*, 74–92.

Smith, R. L. 1978. Poleward propagating perturbations in sea level and currents along the Peru coast. J. Geophys. Res., *83*, 6083–6092.

Received: *22 January, 1981;* revised: *22 October, 1981.*